Finite-Volume Stability and Flux Sectors in a Reciprocal Ratio Gradient Model on Graphs

Anil Thapa*[1] and Jonathan Washburn†[1]

[1]Recognition Physics Research Institute, Austin, Texas 78701, USA

Abstract

We study the finite-volume nearest-neighbor energy generated by the symmetric reciprocal-ratio penalty and its logarithmic representation as a gradient model with potential $V(t) = \cosh t - 1$. We separate general convex structure from formulas specific to this hyperbolic potential. For an oriented nearest-neighbor energy, the gradient form gives a weighted-Laplacian Hessian, while a global lower-curvature bound $W'' \geq \kappa > 0$ yields strong convexity after removal of the constant mode, spectral-gap coercivity, unique minimizers on fixed-mean slices, unique minimizing edge representatives in fixed-flux sectors, and quadratic stability gaps. On coordinate-constant twisted tori, strict convexity already forces affine minimizers and gives the exact energy density $\sum_i W(a_i)$. What is specific to the reciprocal-ratio model is the elementary hyperbolic form $W' = \sinh$, $W'' = \cosh$: the sector equation becomes $\delta \sinh \omega = 0$, the cycle calculation is explicit, and the twisted energy density is $\sum_i (\cosh a_i - 1)$. For boxes and discrete tori in $\mathbb{Z}^d$, explicit spectral gaps yield, in $d = 3$, an $o(L)$ sufficient condition for the normalized logarithmic field to vanish in averaged L^2. Our analysis is carried out in finite volume on fixed graphs with prescribed boundary, mean, or flux data. At positive temperature, we formulate the corresponding height Gibbs measures on mean-fixed slices within each flux sector and describe explicitly how they transform under a change of sector representative.

1 Introduction

Local edge energies built from disagreement variables are basic objects in variational statistical mechanics, lattice interface theory, and network dynamics. In additive models one penalizes differences $r_v - r_w$. In multiplicative models the natural observable is instead a ratio x_v/x_w. Variational, convex-analytic, and equilibrium formulations of such lattice systems are classical in rigorous statistical mechanics and large-deviation theory.[1–6]

Gradient models are effective field descriptions, not Newtonian particle systems: the basic variable is a height or displacement field and the energy depends on neighboring increments. Classical realizations include fluctuating interfaces separating phases, crystal-surface heights, and displacement fields in anharmonic crystals. Their positive-temperature versions lead to gradient Gibbs measures, random conductance representations, hydrodynamic limits, and Gaussian-free-field scaling questions.[7–13] Height representations also occur in quantum many-body problems, for example at Rokhsar–Kivelson-type quantum critical points, but there the height field encodes a quantum ground-state wave functional or an effective Euclidean theory.[14] The model studied below is strictly a classical, zero-temperature finite-volume energy. Here and throughout, *deterministic* is used in the configuration-wise variational sense: once the finite graph and boundary, mean, or flux

*Electronic mail: athapa@recognitionphysics.org
†Electronic mail: jon@recognitionphysics.org

data are fixed, the conclusions are exact statements about energies, minimizers, and inequalities, with no random input, thermal sampling, or stochastic dynamics. The word is not being used in the theory-of-computation sense, and it does not assert that every field variable is a directly measurable physical entity; any such physical interpretation depends on the application. The quantum examples motivate the breadth of height-field language but are not claimed as applications of the present theorems.

In this paper, we study the reciprocal ratio cost

$$J(x) = \frac{1}{2}\left(x + x^{-1}\right) - 1, \qquad x > 0, \tag{1}$$

and the associated graph energy

$$C_G[x] = \sum_{\langle v,w\rangle \in E} J\left(\frac{x_v}{x_w}\right). \tag{2}$$

The energy is invariant under global rescaling $x \mapsto cx$, and in logarithmic variables $r_v = \ln x_v$ it becomes

$$F_G[r] := C_G[e^r] = \sum_{\langle v,w\rangle \in E} \big(\cosh(r_v - r_w) - 1\big). \tag{3}$$

Thus the model is a nearest-neighbor gradient system with edge potential $V(t) = \cosh t - 1$. Since $V''(t) = \cosh t \geq 1$, it satisfies the global lower-curvature assumption used in Brascamp–Lieb inequalities and in the theory of gradient Gibbs or interface models.[7–9, 15–17] Near consensus one has $V(t) = \frac{1}{2}t^2 + O(t^4)$, so the small-fluctuation regime is governed by the usual graph Dirichlet energy and its spectral-gap estimates.[18–21]

More precisely, in finite-dimensional convex analysis $V'' \geq 1$ means that V is globally 1-strongly convex. Because "uniform convexity" has competing conventions, we state the one-sided hypothesis $W'' \geq \kappa > 0$ directly; phrases such as uniform lower curvature or uniform strict convexity, when used, refer only to this quadratic lower bound. No matching upper-curvature bound is assumed: $V''(t) = \cosh t$ is unbounded, so no two-sided uniform ellipticity is claimed. Broader modulus-based notions of uniform convexity, which can produce nonquadratic rates and exponents, are not used here.

The transformation from (2) to (3) has four elementary steps. First, positivity of x_v makes $r_v = \ln x_v$ a real, hence noncompact, field. Second, multiplicative ratios linearize as $x_v/x_w = e^{r_v - r_w}$. Third, the reciprocal symmetry $J(x) = J(x^{-1})$ becomes the evenness $V(t) = V(-t)$. Fourth, the special algebraic choice

$$J(x) = \frac{(x-1)^2}{2x} \tag{4}$$

gives $V(t) = J(e^t) = \cosh t - 1$, with $V(0) = V'(0) = 0$ and $V''(t) \geq 1$. Thus the assumptions in the ratio formulation match exactly the shift symmetry, noncompact target, and lower curvature used in the gradient formulation. The particular cost is motivated by inversion symmetry, nonnegativity with a unique minimum at equality, divergence for both extreme ratios, quadratic response near consensus, and the fact that both V and V' remain explicit. Physically, it is used here as a phenomenological relative-mismatch energy: it is harmonic for small logarithmic strain and becomes increasingly stiff for large strain. No microscopic derivation or unique selection principle is claimed.

The logarithmic formulation also gives the model a direct physical reading. The original variables $x_v > 0$ may be viewed as positive local amplitudes or scale variables attached to the vertices, and the reciprocal-ratio penalty measures relative mismatch across an edge rather than additive discrepancy.

Passing to $r_v = \ln x_v$ turns this multiplicative disagreement into an additive height difference, with the global rescaling symmetry $x \mapsto cx$ becoming the global height-shift symmetry $r \mapsto r + (\ln c)\mathbf{1}$. In this sense the model is a zero-temperature noncompact interface model with explicit strictly convex nearest-neighbor potential $V(t) = \cosh t - 1$. The main point of the paper is that this multiplicative-to-additive change of variables makes the finite-volume sector structure and coercive estimates completely explicit.

The exact logarithmic representation (3) has four concrete finite-volume consequences, but only their explicit hyperbolic form is model-specific. First, the nearest-neighbor gradient structure makes the Hessian a weighted graph Laplacian; the lower bound $W'' \geq \kappa > 0$ then gives strong convexity after removal of the shift mode and spectral-gap coercivity. Second, fixing an oriented edge field h modulo exact shifts $h \sim h + d\phi$ produces a flux-sector problem. Under the same lower-curvature hypothesis, existence, uniqueness, and the quadratic sector gap are general; the Euler–Lagrange equation is $\delta W'(\omega) = 0$. The reciprocal-ratio model makes this the closed nonlinear equation $\delta \sinh \omega = 0$. Theorem 4.2, introduced here as a central result, states the result for the present model. Third, explicit graph spectral gaps turn the general coercive estimate into concrete bounds on boxes and tori, including an $o(L^{d-2})$ sufficient condition for averaged L^2 convergence. Fourth, strict convexity alone makes affine fields minimize coordinate-constant twisted-torus sectors and gives the value $\sum_i W(a_i)$; the special cosh form turns this into the elementary expression $\sum_i(\cosh a_i - 1)$ and gives a closed hyperbolic stationarity equation.

Accordingly, the results are organized to keep the distinction visible. Proposition 2.1 states the general lower-curvature mechanism. Sections 3 and 5 apply it to deterministic stability and explicit graph geometries. Section 4 isolates the sector theorem, gives a worked cycle example, and records representative-aware, mean-fixed finite-volume Gibbs laws. Section 6 first states the general strictly convex principle within the coordinate-constant torus family and then specializes it to $V(t) = \cosh t - 1$. The genuinely model-specific formulas are the sinh coclosed equation, the closed comparison factor $A(M)$, the elementary hyperbolic sector energies, and the compact one-edge reduction in Appendix B.

From the viewpoint of the gradient-Gibbs literature, the flux-sector discussion below is a deterministic finite-graph analogue of working at fixed slope or tilt. Positive-temperature fluctuations, stochastic dynamics, homogenization, and infinite-volume limits belong to a much larger theory.[7–13, 15–17, 22] The present paper uses the term *stability*, not rigidity, because it proves that finite-volume energy controls distance to a minimizing manifold; it does not prove an infinite-volume classification theorem.

A separate but related construction concerns compact phase reduction. Reducing the logarithmic target space modulo $\ln b$ at each site yields a circle-valued field and a one-edge periodic interaction in closed form. Appendix B is included as an additional structural comparison, not as an ingredient in the noncompact theorems: it shows exactly where an edgewise compact reduction loses the global cycle constraints retained by the graph-level quotient. It may serve as a starting point for a future finite-temperature compact model, but no such Gibbs or thermodynamic-limit analysis is claimed here.

The principal results remain finite-volume and zero-temperature. To connect them accurately to the probabilistic literature, Sec. 4.1 defines representative-aware, mean-fixed height laws and the canonical edge-gradient law in each flux sector; infinite-volume DLR existence or uniqueness is not asserted. Section 2 records the general lower-curvature mechanism and the special hyperbolic identities. Section 3 proves strong convexity and quantitative stability. Section 4 establishes the unique minimizing representative in each cohomology class and illustrates it on a cycle. Section 5 gives explicit zero-sector bounds for boxes and tori in $\mathbb{Z}^d$, and Sec. 6 separates the general affine-minimizer principle from the exact reciprocal-ratio formula. The appendices contain the product spectra and the independent compact-phase comparison.

2 The logarithmic formulation and basic comparison estimates

Let $G = (V, E)$ be a simple graph, finite or countably infinite. A configuration is a positive field $x\colon V \to \mathbb{R}_{>0}$. For finite graphs the energy (2) is well defined. On infinite graphs we work only through finite-volume restrictions. The ratio form makes the global scale symmetry immediate:

$$C_G[cx] = C_G[x], \qquad c > 0. \tag{5}$$

In logarithmic variables this becomes the additive symmetry $r \mapsto r + (\ln c)\mathbf{1}$.

For a finite graph and a vertex function $f \in \mathbb{R}^V$, the combinatorial Laplacian is

$$(L_G f)(v) := \sum_{w\,:\,\langle v,w\rangle \in E} \big(f(v) - f(w)\big), \tag{6}$$

and the associated Dirichlet form is

$$\mathcal{E}_G[r] := \frac{1}{2} \sum_{\langle v,w\rangle \in E} (r_v - r_w)^2. \tag{7}$$

We write $d_G(v, w)$ for graph distance and, when G is finite, $\mathrm{diam}(G) = \max_{v,w\in V} d_G(v, w)$ for the graph diameter. Standard references on graph Laplacians and discrete Dirichlet forms include Refs. [18–20]. The purpose of this section is to record the elementary comparison estimates that later drive the coercive bounds and sector analysis.

We first state the part that is independent of the reciprocal-ratio choice. For a finite graph G, fix one orientation $E^{\to}$ containing exactly one orientation $e = (v, w)$ of each undirected edge, set $(dr)(e) := r_w - r_v$, and, for $W \in C^2(\mathbb{R})$, define

$$\mathcal{F}_{G,W}[r] := \sum_{e\in E^{\to}} W\big((dr)(e)\big). \tag{8}$$

The orientation is part of the definition for a general W; if W is even, as in the reciprocal-ratio model, the value is orientation-independent. For a vertex field r, write $\bar{r} := |V|^{-1} \sum_{v\in V} r_v$; when G is connected and $|V| \geq 2$, let $\lambda_2(G) > 0$ denote the smallest nonzero eigenvalue of L_G.

Proposition 2.1 (General lower-curvature mechanism)**.** *Assume that G is connected, $|V| \geq 2$, and $W''(t) \geq \kappa > 0$ for every $t \in \mathbb{R}$. Then, for every $r, \eta \in \mathbb{R}^V$,*

$$D^2\mathcal{F}_{G,W}[r](\eta, \eta) \geq \kappa \sum_{e\in E^{\to}} \big((d\eta)(e)\big)^2. \tag{9}$$

The restriction of $\mathcal{F}_{G,W}$ to every affine slice of fixed vertex mean is $\kappa\lambda_2(G)$-strongly convex. If also $W(0) = W'(0) = 0$, then

$$\mathcal{F}_{G,W}[r] \geq \kappa\mathcal{E}_G[r] \geq \frac{\kappa\lambda_2(G)}{2} \sum_{v\in V} (r_v - \bar{r})^2. \tag{10}$$

More generally, if r_* is stationary modulo constants, then

$$\mathcal{F}_{G,W}[r_* + \eta] - \mathcal{F}_{G,W}[r_*] \geq \frac{\kappa}{2} \sum_{e\in E^{\to}} \big((d\eta)(e)\big)^2. \tag{11}$$

Given an oriented edge field $h = (h_e)_{e \in E^{\to}}$, define the sector energy

$$\mathcal{F}_{G,h,W}[u] := \sum_{e \in E^{\to}} W\big(h_e + (du)(e)\big). \tag{12}$$

It has a unique mean-zero minimizer $u_{h,W}$, and its minimizer at mean m is $u_{h,W} + m\mathbf{1}$. For every $u \in \mathbb{R}^V$, with $\eta := u - u_{h,W}$ and $\bar{\eta} := |V|^{-1} \sum_v \eta_v$,

$$\mathcal{F}_{G,h,W}[u] - \mathcal{F}_{G,h,W}[u_{h,W}] \geq \frac{\kappa}{2} \sum_{e \in E^{\to}} \big((d\eta)(e)\big)^2 \tag{13}$$

$$\geq \frac{\kappa \lambda_2(G)}{2} \sum_{v \in V} (\eta_v - \bar{\eta})^2. \tag{14}$$

Proof. Differentiation gives

$$D^2 \mathcal{F}_{G,W}[r](\eta, \eta) = \sum_{e \in E^{\to}} W''\big((dr)(e)\big)\big((d\eta)(e)\big)^2,$$

which proves (9). On $\mathbf{1}^{\perp}$, the graph Poincaré inequality gives $\sum_{e \in E^{\to}} ((d\eta)(e))^2 \geq \lambda_2(G) \sum_v \eta_v^2$. Taylor's theorem and $W'' \geq \kappa$ give $W(a+s) \geq W(a) + W'(a)s + \frac{\kappa}{2}s^2$. Taking $a = 0$ gives (10); taking a edgewise at a stationary field makes the summed linear term vanish and gives (11). For the sector energy, the identical Hessian bound on a fixed-mean slice is positive definite and coercive, so it gives the stated unique minimizer. Taylor expansion about that stationary minimizer, followed by the graph Poincaré inequality, gives (13)–(14). Notice that the origin-based estimate (10) requires $W(0) = W'(0) = 0$; it is the minimizer-centered gap, not that origin-based estimate, that transfers to an arbitrary sector. □

For $W(t) = \cosh t - 1$, one may take $\kappa = 1$. Thus the lower curvature, spectral-gap scale, and uniqueness consequences in Secs. 3–5 are instances of Proposition 2.1; the following identities retain the extra information specific to cosh.

Lemma 2.2 (Elementary identities for the reciprocal cost)**.** *For $x > 0$ and $t \in \mathbb{R}$, the function J satisfies:*

1.
$$J(x) = \frac{(x-1)^2}{2x} = \frac{1}{2}\left(\sqrt{x} - \frac{1}{\sqrt{x}}\right)^2 \geq 0, \tag{15}$$
with equality if and only if $x = 1$;

2. $J(x) = J(x^{-1})$;

3. $J(e^t) = \cosh t - 1$;

4.
$$\cosh t - 1 \geq \frac{1}{2}t^2 \qquad (t \in \mathbb{R}). \tag{16}$$

Proof. The algebraic identities are immediate. For (16), set $f(t) = \cosh t - 1 - \frac{1}{2}t^2$. Then $f(0) = f'(0) = 0$ and $f''(t) = \cosh t - 1 \geq 0$, so f attains its minimum at $t = 0$. □

The lower bound (16) is the basic bridge from the nonquadratic ratio model to the graph Dirichlet form.

Proposition 2.3 (Dirichlet lower bound)**.** *For every finite graph G and every configuration $x\colon V \to \mathbb{R}_{>0}$ with logarithmic field $r_v = \ln x_v$,*

$$C_G[x] = F_G[r] \geq \mathcal{E}_G[r]. \tag{17}$$

If G is connected, equality holds if and only if r is constant.

Proof. Apply Lemma 2.2(iv) to each edge term in (3). Equality in (16) holds only at $t = 0$, so equality in (17) forces $r_v - r_w = 0$ on every edge. Connectedness then implies that r is constant. □

For a variation direction $\eta \in \mathbb{R}^V$, we use the directional notation $DF_G[r](\eta) := \frac{d}{ds} F_G[r + s\eta]\Big|_{s=0}$ and $D^2F_G[r](\eta, \eta) := \frac{d^2}{ds^2} F_G[r + s\eta]\Big|_{s=0}$. In particular, the symbol η always denotes a test direction in vertex-function space.

Lemma 2.4 (Gradient and Hessian)**.** *Let G be finite. For $r, \eta \in \mathbb{R}^V$,*

$$\big(\nabla F_G[r]\big)_v = \sum_{w\,:\,\langle v,w\rangle \in E} \sinh(r_v - r_w), \tag{18}$$

and

$$D^2F_G[r](\eta, \eta) = \sum_{\langle v,w\rangle \in E} \cosh(r_v - r_w)(\eta_v - \eta_w)^2. \tag{19}$$

Equivalently, the Hessian is the weighted Laplacian with conductances

$$a_{vw}(r) := \cosh(r_v - r_w) \geq 1. \tag{20}$$

In particular,

$$D^2F_G[r](\eta, \eta) \geq 2\mathcal{E}_G[\eta] \qquad (r, \eta \in \mathbb{R}^V). \tag{21}$$

Proof. Differentiate the curve $s \mapsto F_G[r + s\eta]$ once and twice at $s = 0$. Formula (21) follows from (19) and $\cosh \geq 1$. □

Proposition 2.5 (Bounded-gradient comparison)**.** *For $M \geq 0$, define*

$$A(M) := \begin{cases} 1, & M = 0, \\ \dfrac{2(\cosh M - 1)}{M^2}, & M > 0. \end{cases} \tag{22}$$

If a logarithmic field satisfies $|r_v - r_w| \leq M$ on every edge, then

$$\mathcal{E}_G[r] \leq F_G[r] \leq A(M)\, \mathcal{E}_G[r]. \tag{23}$$

Moreover,

$$A(M) = 1 + \frac{M^2}{12} + O(M^4) \qquad (M \to 0). \tag{24}$$

Proof. The lower bound is Proposition 2.3. For $|t| \leq M$ and $M > 0$,

$$\cosh t - 1 = \sum_{k\geq 1} \frac{t^{2k}}{(2k)!} \leq \frac{t^2}{M^2} \sum_{k\geq 1} \frac{M^{2k}}{(2k)!} = \frac{\cosh M - 1}{M^2}\, t^2.$$

Summing over edges yields the upper bound. The expansion (24) is the Taylor series of $\cosh M$. □

Lemma 2.6 (Tangent-plus-quadratic lower bound)**.** *For all $a, s \in \mathbb{R}$,*

$$\cosh(a+s) - 1 \geq \cosh a - 1 + (\sinh a)s + \frac{1}{2}s^2. \tag{25}$$

Equality holds if and only if $s = 0$.

Proof. Set

$$g_a(s) := \cosh(a+s) - 1 - \big(\cosh a - 1\big) - (\sinh a)s - \frac{1}{2}s^2.$$

Then $g_a(0) = g_a'(0) = 0$ and $g_a''(s) = \cosh(a+s) - 1 \geq 0$. Taylor's theorem with integral remainder gives

$$g_a(s) = s^2 \int_0^1 (1-\tau)\big(\cosh(a+\tau s) - 1\big)\, d\tau \geq 0,$$

which proves (25). If $s \neq 0$, then $\tau \mapsto a + \tau s$ ranges over a nondegenerate interval, while $\cosh t - 1$ vanishes only at $t = 0$; hence the integrand is positive on a set of positive measure, so the inequality is strict. Therefore equality holds if and only if $s = 0$. □

Propositions 2.3 and 2.5, together with Lemma 2.6, provide the basic comparison estimates used in the finite-volume analysis below.

3 Finite connected graphs: strong convexity, coercivity, and quantitative stability

In this section $G = (V, E)$ is finite and connected. Write $|V| = N$ and

$$\bar{r} := \frac{1}{N}\sum_{v \in V} r_v. \tag{26}$$

For $m \in \mathbb{R}$, define the affine slice

$$\mathcal{H}_m := \left\{ r \in \mathbb{R}^V : \frac{1}{N}\sum_{v \in V} r_v = m \right\}. \tag{27}$$

The decomposition $\mathbb{R}^V = \mathbb{R}\mathbf{1} \oplus \mathbf{1}^\perp$ shows that fixing the mean removes exactly the global shift mode. Let $\lambda_2(G) > 0$ denote the first nonzero eigenvalue of L_G.

There are two distinct curvature statements here. The edge potential is globally 1-strongly convex on $\mathbb{R}$, but the graph energy is not strongly convex on all of $\mathbb{R}^V$ because constants form its exact zero mode. After restricting to $\mathcal{H}_m$, the incidence operator converts the edge curvature into the vertex-space constant $\lambda_2(G)$. For a general lower bound $W'' \geq \kappa$, every occurrence of $\lambda_2(G)$ below becomes $\kappa\lambda_2(G)$. This is precisely how edgewise curvature drives finite-volume coercivity; the graph geometry supplies the second factor through its Poincaré inequality. No conclusion below requires the broader nonquadratic theory of modulus-based uniform convexity.

Proposition 3.1 (Strong convexity on fixed-mean slices)**.** *For every $m \in \mathbb{R}$, the restriction of F_G to $\mathcal{H}_m$ is $\lambda_2(G)$-strongly convex. Equivalently, for every $r \in \mathcal{H}_m$, every $\eta \in \mathbf{1}^\perp$, and every $s \in \mathbb{R}$,*

$$\frac{d^2}{ds^2} F_G[r + s\eta] \geq \lambda_2(G) \sum_{v \in V} \eta_v^2. \tag{28}$$

Consequently, the unique minimizer of F_G on $\mathcal{H}_m$ is the constant field $r_v \equiv m$.

Proof. By Lemma 2.4,

$$\frac{d^2}{ds^2} F_G[r + s\eta] = D^2 F_G[r + s\eta](\eta, \eta) \geq 2\mathcal{E}_G[\eta].$$

Since $\eta \in \mathbf{1}^{\perp}$, the graph Poincaré inequality gives

$$2\mathcal{E}_G[\eta] \geq \lambda_2(G) \sum_{v \in V} \eta_v^2.$$

This proves (28). The constant field $r_v \equiv m$ belongs to $\mathcal{H}_m$ and has zero energy, hence it is the unique minimizer. □

Proposition 3.2 (Global coercive bound after gauge fixing)**.** *For every* $r \in \mathbb{R}^V$*,*

$$F_G[r] \geq \mathcal{E}_G[r] \geq \frac{\lambda_2(G)}{2} \sum_{v \in V} (r_v - \bar{r})^2. \tag{29}$$

Equivalently, for every $x \colon V \to \mathbb{R}_{>0}$*,*

$$C_G[x] \geq \frac{\lambda_2(G)}{2} \sum_{v \in V} (\ln x_v - \bar{r})^2. \tag{30}$$

Proof. The first inequality is Proposition 2.3. The second is the spectral-gap inequality applied to $r - \bar{r}\,\mathbf{1} \in \mathbf{1}^{\perp}$. □

Remark 3.3*.* At positive temperature the same Hessian lower bound makes the mean-fixed finite-volume law strongly log-concave and yields Brascamp–Lieb variance estimates. Section 4.1 states this sector-wise measure precisely. Proposition 3.2 is its zero-temperature deterministic counterpart.[15, 16]

Corollary 3.4 (Finite-volume ground states)**.** *The finite-volume ground states of the ratio energy are exactly the constant configurations:*

$$C_G[x] = 0 \quad \Longleftrightarrow \quad x_v \equiv c \text{ on } V \text{ for some } c > 0. \tag{31}$$

Equivalently, the ground-state manifold is the global scale orbit of a constant configuration.

Proof. Constant configurations have zero energy. Conversely, if $C_G[x] = 0$, then (15) forces $x_v = x_w$ on every edge, hence on all of V by connectedness. □

Theorem 3.5 (Quantitative stability from total energy)**.** *Let* $x \colon V \to \mathbb{R}_{>0}$ *be a configuration and let* $r_v = \ln x_v$*. Define*

$$\rho_x(v, w) := \sqrt{2\, d_G(v, w)\, C_G[x]}, \qquad R_x := \sqrt{2\, \mathrm{diam}(G)\, C_G[x]}. \tag{32}$$

Then

$$C_G[x] \geq \frac{\lambda_2(G)}{2} \sum_{v \in V} (r_v - \bar{r})^2, \tag{33}$$

$$|r_v - r_w| \leq \rho_x(v, w) \qquad (v, w \in V), \tag{34}$$

$$e^{-\rho_x(v,w)} \leq \frac{x_v}{x_w} \leq e^{\rho_x(v,w)} \qquad (v, w \in V), \tag{35}$$

$$\max_{v,w \in V} |r_v - r_w| \leq R_x, \tag{36}$$

$$\max_{v \in V} |r_v - \bar{r}| \leq R_x, \tag{37}$$

$$e^{-R_x} \leq e^{-\bar{r}} x_v \leq e^{R_x} \qquad (v \in V). \tag{38}$$

Proof. Equation (33) is Proposition 3.2. For (34), let $v = v_0, v_1, \dots, v_m = w$ be a shortest path, so $m = d_G(v, w)$. By Cauchy–Schwarz,

$$\begin{aligned} |r_v - r_w|^2 &= \left| \sum_{i=0}^{m-1} (r_{v_i} - r_{v_{i+1}}) \right|^2 \\ &\le m \sum_{i=0}^{m-1} (r_{v_i} - r_{v_{i+1}})^2 \\ &\le m \sum_{\langle u,u' \rangle \in E} (r_u - r_{u'})^2 = 2m\, \mathcal{E}_G[r] \\ &\le 2m\, C_G[x], \end{aligned}$$

where the last step is Proposition 2.3. This proves (34), and (35) follows by exponentiation. Maximizing (34) over pairs gives (36). For (37),

$$|r_v - \bar{r}| = \left| \frac{1}{N} \sum_{w \in V} (r_v - r_w) \right| \le \frac{1}{N} \sum_{w \in V} |r_v - r_w| \le \max_{w \in V} |r_v - r_w|.$$

Applying (36) proves (37), and (38) is again the exponential form. □

Remark 3.6. The quantities $\rho_x(v, w)$ and R_x package the pathwise and diameter-scale pointwise consequences of the total-energy bound. They are not needed later in the paper, but they record the direct ratio and sup-norm control that follows from the same energy estimate without additional spectral input.

The ground-state characterization and the coercive estimates of this section are not special to the cosh potential: any nonnegative edge cost with a unique zero and a globally lower-bounded logarithmic Hessian gives analogous finite-volume stability statements. What is special here is that the exact logarithmic form (3) keeps the nonlinear stationarity equation and the sector energies explicit. The next sections exploit that extra explicitness to identify the coclosed representative $\delta \sinh \omega = 0$, compute twisted-torus surface tensions exactly, and compare the local compact reduction with the full graph-level quotient.

4 Flux sectors on arbitrary finite graphs

Theorem 4.2 is the central structural result of the paper. It states that after a graph-cohomology class has been fixed, minimization over exact shifts selects one edge field uniquely—not merely a vertex potential up to constants. Fixing a class is the finite-graph analogue of prescribing background cycle flux or macroscopic tilt, and the theorem identifies the preferred representative and its quantitative stability gap. For a general differentiable potential the stationarity equation is $\delta W'(\omega) = 0$; for the reciprocal-ratio potential it becomes $\delta \sinh \omega = 0$. The formalism later specializes to a translation-invariant family of torus sectors in Sec. 6.

The point of the flux-sector formalism is to separate the additive gauge freedom from the cycle data carried by the graph. We use u rather than r for the vertex variable in this section to emphasize that we are now minimizing inside a fixed cohomology class of edge fields. Choose once and for all an orientation $E^{\rightarrow}$ of the edges of a finite connected graph $G = (V, E)$, and write

$$C^0(G) := \mathbb{R}^V, \qquad C^1(G) := \mathbb{R}^{E^{\rightarrow}}. \tag{39}$$

We retain the notation

$$\mathcal{H}_m := \left\{ u \in C^0(G) : \frac{1}{|V|} \sum_{v \in V} u_v = m \right\} \qquad (m \in \mathbb{R}) \tag{40}$$

for the fixed-mean slices. For $u \in C^0(G)$ and $\omega \in C^1(G)$, define the coboundary and divergence by

$$(du)(e) := u(e_+) - u(e_-), \tag{41}$$

$$(\delta\omega)(v) := \sum_{e_+ = v} \omega(e) - \sum_{e_- = v} \omega(e), \tag{42}$$

where e_- and e_+ denote the tail and head of the oriented edge e. We use both $u(v)$ and u_v for the value of a vertex field at v; in particular, $u(e_\pm)$ simply means the value of u at the head or tail of the oriented edge e. Then $\delta d = L_G$, and the discrete integration-by-parts identity

$$\sum_{e \in E^\to} \omega(e)(du)(e) = \sum_{v \in V} (\delta\omega)(v) u_v \tag{43}$$

holds for all $u \in C^0(G)$ and $\omega \in C^1(G)$. We use only this elementary cochain language of finite graphs; see, for example, Refs. [18, 20, 23].

Fix a sector representative $h \in C^1(G)$ and define the corresponding flux-sector energy by

$$F_{G,h}[u] := \sum_{e \in E^\to} \big(\cosh(h_e + (du)(e)) - 1 \big), \qquad u \in C^0(G). \tag{44}$$

Changing h by an exact 1-form leaves the sector unchanged.

Proposition 4.1 (Exact-shift equivalence)**.** *If $\phi \in C^0(G)$ and $h' := h + d\phi$, then*

$$F_{G,h'}[u] = F_{G,h}[u + \phi] \qquad (u \in C^0(G)). \tag{45}$$

Consequently, the minimum of (44) *depends only on the cohomology class*

$$[h] \in H^1(G; \mathbb{R}) := C^1(G)/dC^0(G). \tag{46}$$

Proof. Since $d(u + \phi) = du + d\phi$, one has $h' + du = h + d(u + \phi)$ edgewise, which is exactly (45). The class dependence follows immediately. □

For connected G, the standard edge inner product gives $C^1(G) = dC^0(G) \oplus \ker \delta$. It canonically identifies the quotient $H^1(G; \mathbb{R}) = C^1(G)/dC^0(G)$ with the cycle space $\ker \delta$ and gives $\dim H^1(G; \mathbb{R}) = |E| - |V| + 1$; the quotient and the representative subspace are identified, not literally equal.

Theorem 4.2 (Unique minimizing representative in each flux sector)**.** *Let G be finite and connected, and let $h \in C^1(G)$. Define the sector minimum by*

$$\sigma_G([h]) := \inf_{u \in C^0(G)} F_{G,h}[u]. \tag{47}$$

Then the following hold.

1. *For every $m \in \mathbb{R}$, the restriction of $F_{G,h}$ to the slice $\mathcal{H}_m$ is $\lambda_2(G)$-strongly convex. In particular, on each slice there is a unique minimizer, and the minimizers on different slices differ only by additive constants.*

2. If $u_h \in \mathcal{H}_0$ is the unique mean-zero minimizer and

$$\omega_h := h + du_h \in [h], \tag{48}$$

then

$$\delta \sinh \omega_h = 0. \tag{49}$$

Moreover, ω_h is the unique representative of the class $[h]$ satisfying (49)*.*

3. For every $u \in C^0(G)$, with $\eta := u - u_h$ and $\bar\eta := |V|^{-1} \sum_{v\in V} \eta_v$,

$$F_{G,h}[u] - \sigma_G([h]) \geq \frac{1}{2} \sum_{e\in E^{\to}} (d\eta)(e)^2 \tag{50}$$

$$\geq \frac{\lambda_2(G)}{2} \sum_{v\in V} (\eta_v - \bar\eta)^2. \tag{51}$$

Hence each cohomology class contains a unique energy-minimizing edge representative*; the corresponding vertex potential is unique modulo additive constants.*

Proof. For $u, \zeta \in C^0(G)$,

$$D^2 F_{G,h}[u](\zeta,\zeta) = \sum_{e\in E^{\to}} \cosh\bigl(h_e + (du)(e)\bigr)\,(d\zeta)(e)^2. \tag{52}$$

Since $\cosh \geq 1$, one has

$$D^2 F_{G,h}[u](\zeta,\zeta) \geq \sum_{e\in E^{\to}} (d\zeta)(e)^2 = 2\mathcal{E}_G[\zeta]. \tag{53}$$

If $\zeta \in \mathbf{1}^{\perp}$, the graph Poincaré inequality gives $2\mathcal{E}_G[\zeta] \geq \lambda_2(G) \sum_v \zeta_v^2$, so $F_{G,h}|_{\mathcal{H}_m}$ is $\lambda_2(G)$-strongly convex. In finite dimension, strong convexity implies coercivity on each affine slice and therefore existence and uniqueness of a minimizer. Since adding a constant to u leaves du unchanged, the minimizers on different slices differ only by constants.

Let $u_h \in \mathcal{H}_0$ be the mean-zero minimizer and set $\omega_h = h + du_h$. Because $F_{G,h}[u + c\mathbf{1}] = F_{G,h}[u]$ for every $c \in \mathbb{R}$, the slice minimizer is stationary under arbitrary variations: any $\zeta \in C^0(G)$ decomposes as $(\zeta - \bar\zeta\,\mathbf{1}) + \bar\zeta\,\mathbf{1}$, and the constant part does not change the energy. Differentiating (44) at u_h in the direction $\zeta \in C^0(G)$ gives

$$0 = \frac{d}{ds} F_{G,h}[u_h + s\zeta]\bigg|_{s=0} = \sum_{e\in E^{\to}} \sinh\bigl(\omega_h(e)\bigr)(d\zeta)(e) = \sum_{v\in V} (\delta \sinh \omega_h)(v)\zeta_v,$$

where the last step is (43). Since this holds for every ζ, (49) follows.

Now let $\omega' \in [h]$ also satisfy $\delta \sinh \omega' = 0$. Then $\omega' - \omega_h = d\phi$ for some $\phi \in C^0(G)$. Using (43) again,

$$\begin{aligned} 0 &= \sum_{v\in V} \phi_v \left(\delta\bigl(\sinh\omega' - \sinh\omega_h\bigr)\right)(v) \\ &= \sum_{e\in E^{\to}} (d\phi)(e) \left(\sinh\omega'(e) - \sinh\omega_h(e)\right) \\ &= \sum_{e\in E^{\to}} \left(\omega'(e) - \omega_h(e)\right) \left(\sinh\omega'(e) - \sinh\omega_h(e)\right). \end{aligned}$$

Because sinh is strictly increasing, every summand is nonnegative and vanishes only when $\omega'(e) = \omega_h(e)$. Hence $\omega' = \omega_h$, proving uniqueness of the nonlinear coclosed representative.

Finally, let $u \in C^0(G)$ and set $\eta = u - u_h$. Apply Lemma 2.6 edgewise with $a = \omega_h(e)$ and $s = (d\eta)(e)$:

$$\cosh\bigl(\omega_h(e) + (d\eta)(e)\bigr) - 1 \ge \cosh\bigl(\omega_h(e)\bigr) - 1 + \sinh\bigl(\omega_h(e)\bigr)(d\eta)(e) + \frac{1}{2}(d\eta)(e)^2.$$

Summing over $e \in E^{\to}$ and using (43) together with $\delta \sinh \omega_h = 0$ removes the linear term, which yields (50). Since $d\eta = d(\eta - \bar{\eta}\,\mathbf{1})$, the graph Poincaré inequality gives (51). □

Example 4.3 (A complete cycle calculation)**.** *Let C_q, $q \ge 3$, have consistently oriented edges $e_j = (j, j+1)$, with indices modulo q, and let*

$$H := \sum_{j=0}^{q-1} h_{e_j} \tag{54}$$

be the circulation of a representative h. Exact shifts do not change H, and on a cycle two edge fields are cohomologous exactly when they have the same circulation. Write the minimizing representative as $\omega_j = h_{e_j} + (du_h)(e_j)$. The coclosed equation at vertex j is

$$\sinh \omega_{j-1} = \sinh \omega_j. \tag{55}$$

Since sinh *is strictly increasing, all ω_j are equal. Their sum must be H, so*

$$\omega_j = \frac{H}{q}, \qquad \sigma_{C_q}([h]) = q\left(\cosh \frac{H}{q} - 1\right). \tag{56}$$

For example, on a triangle the minimizing edge field in a sector of circulation H is $(H/3, H/3, H/3)$. The minimizing vertex potential is recovered from the defining identity $\omega_h = h + du_h$:

$$(du_h)(e_j) = \omega_h(e_j) - h_{e_j} = \frac{H}{q} - h_{e_j}. \tag{57}$$

Choose $u_h(0)$ and solve (57) successively. The right-hand side sums to zero, so the construction is consistent after one circuit, and the mean-zero condition fixes the remaining constant. If $H \ne 0$, then ω_h is not exact (its circulation is H); instead, the exact correction $du_h = \omega_h - h$ has zero circulation because ω_h and h represent the same class. For a general differentiable strictly convex potential W, the same computation reads $W'(\omega_{j-1}) = W'(\omega_j)$ and again gives the uniform representative H/q. Thus uniform distribution of circulation is the general convex structure; the hyperbolic-sine equation and the displayed cosh *energy are the model-specific forms.*

Remark 4.4. If G is a tree, every 1-cochain is exact, so $H^1(G; \mathbb{R}) = 0$ and there is only one flux sector. Nontrivial sectors appear precisely when G has cycles. In that sense, Theorem 4.2 is the finite-graph, zero-temperature analogue of working at fixed slope or tilt in gradient Gibbs and interface models.[7, 9, 17]

4.1 Finite-volume Gibbs measures and sector dependence

Although the main theorems are zero-temperature statements, the same curvature gives a precise finite-temperature object. Let $d\lambda_m$ be Lebesgue measure on the affine slice $\mathcal{H}_m$. For inverse temperature $\beta > 0$, a chosen representative $h \in C^1(G)$, and a fixed mean m, define the height-field law

$$\mu^{\beta}_{G,h,m}(du) := \frac{1}{Z^{\beta}_{G,h,m}} \exp\bigl(-\beta F_{G,h}[u]\bigr)\, d\lambda_m(u). \tag{58}$$

Proposition 2.1 and Theorem 4.2 imply Gaussian coercivity about $u_h + m\mathbf{1}$, hence $0 < Z^{\beta}_{G,h,m} < \infty$.

The representative in (58) matters, but only by a natural translation. If $h' = h + d\phi$, put $\phi_0 := \phi - \bar{\phi}\,\mathbf{1}$. Then $F_{G,h'}[u] = F_{G,h}[u + \phi_0]$ on $\mathcal{H}_m$, and therefore

$$\mu^{\beta}_{G,h',m} = \bigl(T_{-\phi_0}\bigr)_{\#}\mu^{\beta}_{G,h,m}, \qquad T_{-\phi_0}(u) := u - \phi_0. \tag{59}$$

The induced edge-gradient law

$$\nu^{\beta}_{G,[h]} := \bigl(u \mapsto h + du\bigr)_{\#}\mu^{\beta}_{G,h,m} \tag{60}$$

is consequently independent of both the chosen representative h and the fixed mean m. Thus $\mu^{\beta}_{G,h,m}$ is the representative-aware height law, while $\nu^{\beta}_{G,[h]}$ is the canonical finite-volume edge-gradient law attached to the class.

The same construction applies to the general sector energy (12); write the resulting law as $\mu^{\beta,W}_{G,h,m}$. If $W'' \geq \kappa > 0$, its density is $\beta\kappa\lambda_2(G)$-strongly log-concave on $\mathcal{H}_m$. In particular, for every $a \in \mathbf{1}^{\perp}$, the Brascamp–Lieb inequality gives the explicit comparison

$$\operatorname{Var}_{\mu^{\beta,W}_{G,h,m}}\left(\sum_{v\in V} a_v u_v\right) \leq \frac{1}{\beta\kappa}\, a^{\mathsf{T}} L_G^{+} a, \tag{61}$$

where L_G^{+} is the Moore–Penrose inverse on $\mathbf{1}^{\perp}$. For $W(t) = \cosh t - 1$, one has $\kappa = 1$. Applying the same variance estimate to exponential tilts, whose Hessian is unchanged, gives the genuine sub-Gaussian moment-generating-function bound

$$\log \mathbb{E}_{\mu^{\beta,W}_{G,h,m}} \exp\left[t\left(\sum_v a_v u_v - \mathbb{E}_{\mu^{\beta,W}_{G,h,m}} \sum_v a_v u_v\right)\right] \leq \frac{t^2}{2\beta\kappa}\, a^{\mathsf{T}} L_G^{+} a \qquad (t \in \mathbb{R}). \tag{62}$$

Corollary 4.5 (Finite-volume zero-temperature concentration)**.** *Let $u_{h,W}$ be the mean-zero minimizer of $\mathcal{F}_{G,h,W}$ and let $W'' \geq \kappa > 0$. Then*

$$\mathbb{E}_{\mu^{\beta,W}_{G,h,m}} \bigl\|u - \bigl(u_{h,W} + m\mathbf{1}\bigr)\bigr\|_2^2 \leq \frac{|V| - 1}{\beta\kappa\lambda_2(G)}. \tag{63}$$

Consequently, for every $\varepsilon > 0$,

$$\mu^{\beta,W}_{G,h,m}\bigl(\bigl\|u - \bigl(u_{h,W} + m\mathbf{1}\bigr)\bigr\|_2 \geq \varepsilon\bigr) \leq \frac{|V| - 1}{\beta\kappa\lambda_2(G)\varepsilon^2} \xrightarrow[\beta\to\infty]{} 0. \tag{64}$$

Proof. Work on the $(|V| - 1)$-dimensional affine space $\mathcal{H}_m$ and set $u_* := u_{h,W} + m\mathbf{1}$. Gaussian coercivity makes the boundary term vanish, so integration by parts against the density in (58), with $F_{G,h}$ replaced by $\mathcal{F}_{G,h,W}$, gives

$$|V| - 1 = \beta\, \mathbb{E}\, \langle u - u_*, \nabla_{\mathcal{H}_m} \mathcal{F}_{G,h,W}[u] \rangle\,.$$

The slice gradient vanishes at u_*, and $\kappa\lambda_2(G)$-strong convexity bounds the inner product below by $\kappa\lambda_2(G)\|u - u_*\|_2^2$. This proves (63); Markov's inequality gives (64). $\square$

Three qualifications prevent a misleading uniqueness claim. First, without fixing a mean or pinning one vertex, integration over the constant mode gives an infinite normalization because $F_{G,h}[u + c\mathbf{1}] = F_{G,h}[u]$. Second, after gauge fixing there is a unique height law for each chosen representative, related to other representatives by (59); equivalently, there is one canonical edge-gradient law (60) per class $[h]$. A graph with cycles has many such classes, and a law mixing sectors requires an additional choice of weights. Third, this finite-volume uniqueness is not an infinite-volume DLR uniqueness theorem.

For the free boxes and periodic tori in Sec. 5, the deterministic results concern the zero sector, and choosing $h = 0$ in (58) supplies the unique mean-fixed height law. For the twisted tori in Sec. 6, one takes the coordinate-constant representative $h = h^a$. A quadratic potential gives an exactly Gaussian field; the present cosh potential does not. It gives a non-Gaussian but strongly log-concave field with the comparison bounds (61)–(62) and the concentration statement in Corollary 4.5. Its unbounded upper curvature should not be confused with exact Gaussianity or with a two-sided uniform-ellipticity hypothesis. Contemporary positive-temperature work treats localization, scaling, and dynamics under additional hypotheses, including settings with unbounded or degenerate curvature.[10–13, 22] Those thermodynamic and dynamical questions remain outside the present finite-volume variational analysis.

5 Boxes and tori in $\mathbb{Z}^d$

We now specialize the finite-volume bounds to the standard cubic boxes in $\mathbb{Z}^d$. Let

$$\Lambda_{L,d} := [-L, L]^d \cap \mathbb{Z}^d, \qquad N_L := 2L + 1, \tag{65}$$

and consider either the free box graph on $\Lambda_{L,d}$ or the periodic torus $(\mathbb{Z}/N_L\mathbb{Z})^d$. For a configuration x on either graph, write $r_v := \ln x_v$ and

$$\bar{r}_{L,d} := \frac{1}{N_L^d} \sum_v r_v, \tag{66}$$

with the sum over the relevant vertex set. The corresponding energies are denoted by $C^{\mathrm{f}}_{L,d}[x]$ and $C^{\mathrm{p}}_{L,d}[x]$.

Lemma 5.1 (Spectral gaps of boxes and tori)**.** *For every $d \geq 1$ and every $L \geq 1$, the Laplacian spectral gaps of the free box and periodic torus are*

$$\lambda^{\mathrm{f}}_{2,d}(L) = 2\left(1 - \cos\frac{\pi}{N_L}\right), \tag{67}$$

$$\lambda^{\mathrm{p}}_{2,d}(L) = 2\left(1 - \cos\frac{2\pi}{N_L}\right). \tag{68}$$

In particular,

$$\lambda^{\mathrm{f}}_{2,d}(L) \geq \frac{4}{N_L^2}, \qquad \lambda^{\mathrm{p}}_{2,d}(L) \geq \frac{16}{N_L^2}. \tag{69}$$

Proof. The box and torus are Cartesian products of d copies of the path graph P_{N_L} and the cycle graph C_{N_L}, respectively. Their Laplacian eigenvalues therefore add. The product formulas are recorded in Appendix A. The smallest positive eigenvalue is obtained by taking one factor in its first nontrivial mode and the remaining factors in the zero mode, which yields (67) and (68). The bounds (69) follow from $1 - \cos t = 2\sin^2(t/2) \geq 2(t/\pi)^2$ for $0 \leq t \leq \pi$. $\square$

Theorem 5.2 (Averaged coercive bounds on boxes and tori)**.** *For every $d \geq 1$, every $L \geq 1$, and every configuration x on the free box, with $r_v := \ln x_v$,*

$$\frac{1}{N_L^d} \sum_{v \in \Lambda_{L,d}} (r_v - \bar{r}_{L,d})^2 \leq \frac{1}{2N_L^{d-2}} \, C^{\mathrm{f}}_{L,d}[x]. \tag{70}$$

For every configuration x on the periodic torus, with $r_v := \ln x_v$,

$$\frac{1}{N_L^d} \sum_{v \in (\mathbb{Z}/N_L\mathbb{Z})^d} (r_v - \bar{r}_{L,d})^2 \leq \frac{1}{8N_L^{d-2}} \, C^{\mathrm{p}}_{L,d}[x]. \tag{71}$$

Consequently, if $\{x^{(L)}\}_{L \geq 1}$ is a sequence of free-boundary configurations such that

$$C^{\mathrm{f}}_{L,d}[x^{(L)}] = o(L^{d-2}) \qquad (L \to \infty), \tag{72}$$

or a sequence of periodic configurations such that

$$C^{\mathrm{p}}_{L,d}[x^{(L)}] = o(L^{d-2}) \qquad (L \to \infty), \tag{73}$$

then, writing

$$\bar{r}^{(L)}_{L,d} := \frac{1}{N_L^d} \sum_v \ln x_v^{(L)}, \tag{74}$$

with the sum over the relevant vertex set, the normalized fields

$$y_v^{(L)} := e^{-\bar{r}^{(L)}_{L,d}} x_v^{(L)} \tag{75}$$

satisfy

$$\frac{1}{N_L^d} \sum_v \big(\ln y_v^{(L)}\big)^2 \longrightarrow 0. \tag{76}$$

Proof. For free boundary conditions, Proposition 3.2 and Lemma 5.1 give

$$\sum_{v \in \Lambda_{L,d}} (r_v - \bar{r}_{L,d})^2 \leq \frac{2}{\lambda^{\mathrm{f}}_{2,d}(L)} \, C^{\mathrm{f}}_{L,d}[x] \leq \frac{N_L^2}{2} \, C^{\mathrm{f}}_{L,d}[x].$$

Dividing by N_L^d yields (70). The periodic estimate (71) is identical, using $\lambda^{\mathrm{p}}_{2,d}(L) \geq 16/N_L^2$. Finally, $\ln y_v^{(L)} = \ln x_v^{(L)} - \bar{r}^{(L)}_{L,d}$, so (76) says precisely that the mean-zero logarithmic field converges to zero in averaged L^2. Since $N_L \sim 2L$, either (72) or (73) implies (76). ☐

Remark 5.3 (Role of curvature in the box and torus estimates)*.* Theorem 5.2 uses only the quadratic lower-curvature constant and the graph spectral gap. If $\cosh t - 1$ is replaced by a potential W with $W(0) = W'(0) = 0$ and $W'' \geq \kappa > 0$, the right-hand sides of (70) and (71) are divided by κ. A more general modulus of uniform convexity would instead require a corresponding nonquadratic coercive inequality; no such extension is invoked in the theorem. At positive temperature, the same κ enters the finite-volume variance bound described in Sec. 4.1.

Remark 5.4 (Three-dimensional scaling)*.* In dimension $d = 3$, (70) and (71) reduce to

$$\frac{1}{N_L^3} \sum_{v \in \Lambda_{L,3}} (r_v - \bar{r}_{L,3})^2 \leq \frac{1}{2N_L} \, C^{\mathrm{f}}_{L,3}[x], \tag{77}$$

and

$$\frac{1}{N_L^3}\sum_{v\in(\mathbb{Z}/N_L\mathbb{Z})^3}(r_v-\bar r_{L,3})^2\le\frac{1}{8N_L}\,C^{\mathrm{p}}_{L,3}[x]. \tag{78}$$

Thus $o(L)$ total energy is a sufficient condition for the mean-zero logarithmic field to converge to zero in box-averaged L^2 after normalization.

Remark 5.5. Theorem 5.2 is a finite-size coercive statement, not an infinite-volume classification theorem. It identifies the scale at which the mean-zero logarithmic field $\ln y^{(L)}$ is forced to converge to zero in averaged L^2, but it does not classify infinite-volume local minimizers or Gibbs states.

6 Twisted torus sectors as an explicit flux-sector specialization

We now specialize Theorem 4.2 to coordinate-constant oriented edge fields on a discrete torus. This is an important restriction: $H^1(T_{N,d};\mathbb{R})=C^1(T_{N,d})/dC^0(T_{N,d})$ is the cohomology of the *graph*. With the standard edge inner product, the orthogonal decomposition above identifies this quotient with the full cycle space $\ker\delta$, which contains microscopic cycle directions in addition to the coordinate windings. The classes $[h^a]$ below form the d-parameter translation-invariant family associated with those windings. When $d=1$, this family exhausts $H^1(C_N;\mathbb{R})$; when $d\ge 2$ and $N\ge 3$, it is a proper subspace because

$$\dim H^1(T_{N,d};\mathbb{R})=|E|-|V|+1=(d-1)N^d+1>d.$$

Thus, except in the one-dimensional cycle case, the slope-vector construction does not exhaust all graph-cohomology sectors. It is singled out because its minimizer and energy are explicit. Outside this d-parameter family, the general sector equation remains $\delta W'(\omega)=0$, generally without an affine closed form.

Let

$$T_{N,d}:=(\mathbb{Z}/N\mathbb{Z})^d,\qquad N\ge 3, \tag{79}$$

and for $u\colon T_{N,d}\to\mathbb{R}$ write

$$\nabla_i u(n):=u(n+e_i)-u(n),\qquad i=1,\dots,d, \tag{80}$$

where e_i is the ith coordinate vector and addition is modulo N. Fix a slope vector $a=(a_1,\dots,a_d)\in\mathbb{R}^d$ and define the twisted torus energy

$$F^{(a)}_{N,d}[u]:=\sum_{n\in T_{N,d}}\sum_{i=1}^{d}\big(\cosh(a_i+\nabla_i u(n))-1\big). \tag{81}$$

Equivalently, if $r\colon\mathbb{Z}^d\to\mathbb{R}$ satisfies the quasi-periodicity condition

$$r(n+Ne_i)=r(n)+Na_i\qquad(i=1,\dots,d), \tag{82}$$

then $r(n)=a\cdot n+u(n)$ with u N-periodic, and the energy on one fundamental cell is exactly (81).

The affine-minimizer mechanism is not peculiar to cosh. To make the division between general structure and explicit specialization precise, let

$$F^{(a)}_{N,d;W}[u]:=\sum_{n\in T_{N,d}}\sum_{i=1}^{d}W(a_i+\nabla_i u(n))\,. \tag{83}$$

Proposition 6.1 (General strictly convex principle for coordinate-constant torus twists)**.** *If $W\colon \mathbb{R} \to \mathbb{R}$ is strictly convex, then*

$$F^{(a)}_{N,d;W}[u] \ge N^d \sum_{i=1}^{d} W(a_i), \tag{84}$$

with equality if and only if u is constant. If, in addition, $W \in C^2(\mathbb{R})$ and $W'' \ge \kappa > 0$, then

$$F^{(a)}_{N,d;W}[u] - N^d \sum_{i=1}^{d} W(a_i) \ge \frac{\kappa}{2} \sum_{n\in T_{N,d}} \sum_{i=1}^{d} \big(\nabla_i u(n)\big)^2 \tag{85}$$

$$\ge \kappa \left(1 - \cos\frac{2\pi}{N}\right) \sum_{n\in T_{N,d}} \big(u(n) - \bar{u}\big)^2. \tag{86}$$

Proof. Periodicity gives $\sum_n \nabla_i u(n) = 0$ for every i. Jensen's inequality therefore yields

$$\frac{1}{N^d} \sum_n W(a_i + \nabla_i u(n)) \ge W\left(a_i + \frac{1}{N^d} \sum_n \nabla_i u(n)\right) = W(a_i).$$

Strict convexity makes equality possible only when $\nabla_i u$ is constant in n; its zero average then gives $\nabla_i u = 0$ for every i, and connectedness makes u constant. If $W'' \ge \kappa$, the tangent-plus-quadratic bound $W(a_i + s) \ge W(a_i) + W'(a_i)s + \frac{\kappa}{2}s^2$ gives (85) after the linear terms telescope. The torus spectral gap gives (86). $\square$

Thus strict convexity is responsible for affine minimization, while the choice $W(t) = \cosh t - 1$ supplies the explicit functions $W(a_i) = \cosh a_i - 1$, $W'(t) = \sinh t$, and the curvature constant $\kappa = 1$.

Theorem 6.2 (Cosh specialization in coordinate-constant twisted sectors)**.** *For every $N \ge 3$, every $d \ge 1$, every slope $a \in \mathbb{R}^d$, and every periodic field $u\colon T_{N,d} \to \mathbb{R}$,*

$$F^{(a)}_{N,d}[u] \ge N^d \sum_{i=1}^{d} \big(\cosh a_i - 1\big), \tag{87}$$

$$F^{(a)}_{N,d}[u] - N^d \sum_{i=1}^{d} \big(\cosh a_i - 1\big) \ge \frac{1}{2} \sum_{n\in T_{N,d}} \sum_{i=1}^{d} \big(\nabla_i u(n)\big)^2 \tag{88}$$

$$\ge \left(1 - \cos\frac{2\pi}{N}\right) \sum_{n\in T_{N,d}} \big(u(n) - \bar{u}\big)^2, \tag{89}$$

where

$$\bar{u} := \frac{1}{N^d} \sum_{n\in T_{N,d}} u(n). \tag{90}$$

Equality in (87) *holds if and only if u is constant. Equivalently, among all quasi-periodic lifts satisfying* (82)*, the unique minimizers modulo additive constants are the affine fields*

$$r(n) = a \cdot n + c. \tag{91}$$

Proof. Orient every torus edge in the positive coordinate direction and define the sector representative $h^a \in C^1(T_{N,d})$ by

$$h^a_{(n,n+e_i)} := a_i, \qquad n \in T_{N,d}, \quad i = 1, \dots, d. \tag{92}$$

Then $F^{(a)}_{N,d}[u] = F_{T_{N,d},h^a}[u]$. At every vertex $n \in T_{N,d}$,

$$(\delta \sinh h^a)(n) = \sum_{i=1}^{d} \sinh(a_i) - \sum_{i=1}^{d} \sinh(a_i) = 0,$$

so h^a already satisfies the Euler–Lagrange condition (49). By Theorem 4.2, it is therefore the unique energy-minimizing representative of its cohomology class, and the unique mean-zero minimizing vertex field is $u_h \equiv 0$. Evaluating the energy at a constant field gives

$$\sigma_{T_{N,d}}([h^a]) = N^d \sum_{i=1}^{d} \bigl(\cosh a_i - 1\bigr),$$

which is exactly (87). The uniqueness statement in Theorem 4.2 shows that equality in (87) holds precisely for constant u, equivalently for affine quasi-periodic lifts (91) modulo additive constants.

For the quantitative gap, apply (50) from Theorem 4.2 with $u_h \equiv 0$:

$$F^{(a)}_{N,d}[u] - N^d \sum_{i=1}^{d} (\cosh a_i - 1) \geq \frac{1}{2} \sum_{n \in T_{N,d}} \sum_{i=1}^{d} \bigl(\nabla_i u(n)\bigr)^2,$$

which is (88). The bound (89) then follows from the torus spectral-gap estimate, whose first nonzero Laplacian eigenvalue is $2(1 - \cos(2\pi/N))$ by (100) and the Cartesian-product formula (103). □

Corollary 6.3 (Exact zero-temperature surface tension)**.** *Define the finite-size twisted energy density by*

$$\sigma_{N,d}(a) := \frac{1}{N^d} \inf_{u\colon T_{N,d} \to \mathbb{R}} F^{(a)}_{N,d}[u]. \tag{93}$$

Then

$$\sigma_{N,d}(a) = \sum_{i=1}^{d} \bigl(\cosh a_i - 1\bigr), \tag{94}$$

so the zero-temperature surface tension is already exact at finite size and does not depend on N. In particular,

$$\sigma_{N,d}(a) = \frac{1}{2}|a|^2 + O(|a|^4) \qquad (a \to 0). \tag{95}$$

Proof. Equation (94) is (87) divided by N^d, with equality achieved by any constant u, equivalently by the affine quasi-periodic lift $r(n) = a \cdot n + c$. The expansion (95) follows from the Taylor series of cosh. □

7 Conclusion

For the reciprocal ratio cost (1), the logarithmic change of variables converts a multiplicative graph interaction into a noncompact height model whose edge potential is globally 1-strongly convex. The full graph functional retains the constant shift as an exact zero mode and becomes strongly convex only after that mode is removed. Proposition 2.1 makes the scope of the general theory explicit: nearest-neighbor gradient structure produces the weighted-Laplacian Hessian, while a global quadratic lower-curvature bound yields spectral-gap coercivity, unique fixed-mean minimizers, unique minimizing edge representatives in fixed sectors, and minimizer-centered quadratic gaps. These are not claimed as consequences peculiar to cosh, and no finite global upper-curvature bound is available for cosh.

What is specific to the present model is the persistence of closed form after the logarithmic transform. For a general differentiable strictly convex potential, a sector minimizer is characterized by $\delta W'(\omega) = 0$; lower curvature gives its quantitative gap. Here this becomes the explicit nonlinear coclosed equation $\delta \sinh \omega = 0$, and the cycle energy has the elementary hyperbolic formula (56). On d-dimensional boxes and tori the graph spectral gaps can be written explicitly, so the general zero-sector coercive estimate becomes a concrete finite-size bound. In dimension three, the resulting L^{-1} scale gives an $o(L)$ sufficient condition under which the normalized logarithmic field vanishes in averaged L^2.

The coordinate-constant twisted torus sectors form a d-parameter family inside $H^1(T_{N,d}; \mathbb{R})$, identified through the standard edge inner product with the full cycle space $\ker \delta$, and exhaust it only for $d = 1$. Proposition 6.1 shows that strict convexity, not the hyperbolic form, is responsible for their affine minimizers; cosh supplies the exact displayed energy $\sum_i (\cosh a_i - 1)$ and the explicit sinh stationarity equation. Section 4.1 defines representative-aware, mean-fixed height laws and the canonical edge-gradient law in each sector, with explicit finite-temperature comparison and zero-temperature concentration bounds. These are finite-volume consequences of the same curvature, not infinite-volume results. Appendix B is an independent structural comparison: its local periodic interaction agrees with the graph-level quotient on trees but can differ on cyclic graphs because edgewise minimization forgets global compatibility. The paper's contribution is therefore a precise finite-volume analysis that distinguishes universal convex consequences from the closed hyperbolic formulas inherited from the reciprocal-ratio origin.

Author Contributions:

Conceptualization, J.W.; methodology, A.T. and J.W.; formal analysis, A.T. and J.W.; writing—original draft preparation, J.W.; writing—review and editing, A.T. and J.W. All authors have read and agreed to the published version of the manuscript.

Acknowledgments

We thank Sebastian Pardo-Guerra, Philip Beltracchi, and Elshad Allahyarov for valuable discussions and feedback. This work utilized the computing and AI resources of the RS Institute.

Data Availability

No new data were generated or analyzed in support of this research.

A Product-spectrum formulas for boxes and tori

This appendix records the spectral calculation used in Lemma 5.1. Fix $d \geq 1$ and set $N = N_L = 2L + 1$.

For the path graph P_N on vertices $\{1, \ldots, N\}$, define

$$u_m(j) := \cos\left(\frac{\pi m}{N}\left(j - \frac{1}{2}\right)\right), \qquad m = 0, 1, \ldots, N-1. \tag{96}$$

A direct computation shows that these are Laplacian eigenvectors with eigenvalues

$$\lambda_m(P_N) = 2\left(1 - \cos\frac{\pi m}{N}\right), \qquad m = 0, 1, \ldots, N-1. \tag{97}$$

In particular, the first nonzero eigenvalue is

$$\lambda_2(P_N) = 2\left(1 - \cos\frac{\pi}{N}\right). \tag{98}$$

For the cycle graph C_N on $\mathbb{Z}/N\mathbb{Z}$, the Fourier modes

$$\psi_k(j) := e^{2\pi i k j/N}, \qquad k = 0, 1, \ldots, N-1, \tag{99}$$

diagonalize the Laplacian with eigenvalues

$$\lambda_k(C_N) = 2\left(1 - \cos\frac{2\pi k}{N}\right). \tag{100}$$

Hence the first nonzero eigenvalue is

$$\lambda_2(C_N) = 2\left(1 - \cos\frac{2\pi}{N}\right). \tag{101}$$

The free box $\Lambda_{L,d}$ is the Cartesian product of d copies of P_N, while the periodic torus $(\mathbb{Z}/N\mathbb{Z})^d$ is the Cartesian product of d copies of C_N. For Cartesian products, Laplacian eigenvalues add. Hence the free-box eigenvalues are

$$\lambda^{\mathrm{f}}_{m_1,\ldots,m_d} = \sum_{i=1}^{d} 2\left(1 - \cos\frac{\pi m_i}{N}\right), \qquad m_i \in \{0, \ldots, N-1\}, \tag{102}$$

and the periodic-torus eigenvalues are

$$\lambda^{\mathrm{p}}_{k_1,\ldots,k_d} = \sum_{i=1}^{d} 2\left(1 - \cos\frac{2\pi k_i}{N}\right), \qquad k_i \in \{0, \ldots, N-1\}. \tag{103}$$

The smallest positive eigenvalue is obtained by taking one coordinate equal to 1 and the remaining coordinates equal to 0, which yields (67) and (68).

B Local phase reduction: reduced edge potential and graph-level quotient

This appendix is included for a specific reason. The main body studies a noncompact gradient model, but the logarithmic variable also admits a natural compact phase obtained by reducing it modulo $\ln b$ sitewise. That local reduction produces an explicit one-edge periodic interaction, so one can build a compact phase energy directly and then compare it with the genuine graph-level quotient over sitewise integer lifts. This operation should be distinguished from quotienting only the global rescaling symmetry, and it is also different from the twisted torus sectors of Sec. 6, where the logarithmic variable remains noncompact but carries a prescribed quasi-periodic slope. On graphs with cycles, the local compact reduction need not coincide with the full graph-level quotient: optimizing edge by edge forgets the global compatibility constraints, or equivalently the cycle data, retained by the graph-level quotient. No theorem in the main text depends on this construction. It is retained as an additional structural result and as a possible point of departure for a future compact, positive-temperature model; such an extension is not analyzed here.

Proposition B.1 (Global quotient versus sitewise phase reduction)**.** *Assume G is finite with $|V| = N$, and fix $b > 1$. Quotienting the logarithmic configuration space $\mathbb{R}^V$ by the global subgroup $(\ln b)\mathbb{Z}\,\mathbf{1}$ gives*

$$\mathbb{R}^V/\big((\ln b)\mathbb{Z}\,\mathbf{1}\big) \cong \mathbf{1}^\perp \times \big(\mathbb{R}/(\ln b)\mathbb{Z}\big). \tag{104}$$

In particular, the global quotient compactifies only the zero mode and leaves the $N-1$ relative directions noncompact. By contrast, reducing each site modulo $\ln b$ gives the phase space

$$\big(\mathbb{R}/(\ln b)\mathbb{Z}\big)^V \cong (\mathbb{R}/\mathbb{Z})^V. \tag{105}$$

Proof. Every $r \in \mathbb{R}^V$ decomposes uniquely as $r = \bar{r}\,\mathbf{1} + r^\perp$ with $r^\perp \in \mathbf{1}^\perp$. Translation by $(\ln b)\mathbb{Z}\,\mathbf{1}$ acts only on the scalar coordinate $\bar{r}$ and leaves $r^\perp$ unchanged, giving (104). Reducing each coordinate modulo $\ln b$ separately yields (105). □

We therefore introduce the phase variable as the class of $r_v/\ln b$ in $\mathbb{R}/\mathbb{Z}$:

$$\Theta_v := \frac{r_v}{\ln b} + \mathbb{Z} \in \mathbb{R}/\mathbb{Z}, \qquad b > 1, \tag{106}$$

and for a phase difference $\delta \in \mathbb{R}$ define the reduced edge potential by minimizing over integer lifts,

$$\widetilde{J}_b(\delta) := \min_{n\in\mathbb{Z}} J\left(b^{n+\delta}\right) = \min_{n\in\mathbb{Z}}\big(\cosh((\ln b)(n+\delta)) - 1\big). \tag{107}$$

Let

$$d_{\mathbb{Z}}(\delta) := \min_{n\in\mathbb{Z}} |\delta - n| \in \left[0, \frac{1}{2}\right] \tag{108}$$

denote the distance to the nearest integer.

Proposition B.2 (Closed form of the reduced periodic interaction)**.** *For every $b > 1$ and every $\delta \in \mathbb{R}$,*

$$\widetilde{J}_b(\delta) = \cosh\big((\ln b)\, d_{\mathbb{Z}}(\delta)\big) - 1. \tag{109}$$

Hence $\widetilde{J}_b$ is even and 1-periodic, satisfies $\widetilde{J}_b \geq 0$, and vanishes if and only if $\delta \in \mathbb{Z}$. It is continuous and piecewise analytic, with nondifferentiable points at the half-integers.

Proof. The map $u \mapsto \cosh((\ln b)u) - 1$ is even and strictly increasing for $u \geq 0$. Therefore the minimizing integer in (107) is the one that makes $|n+\delta|$ minimal, namely $|n+\delta| = d_{\mathbb{Z}}(\delta)$. □

Proposition B.3 (Quadratic bounds for the reduced interaction)**.** *For every $b > 1$ and every $\delta \in \mathbb{R}$,*

$$\frac{(\ln b)^2}{2}\, d_{\mathbb{Z}}(\delta)^2 \leq \widetilde{J}_b(\delta) \leq 4\big(\cosh((\ln b)/2) - 1\big)\, d_{\mathbb{Z}}(\delta)^2. \tag{110}$$

Proof. Set $t = (\ln b)\, d_{\mathbb{Z}}(\delta)$, so $|t| \leq (\ln b)/2$. The lower bound is (16) applied to (109). For the upper bound, apply Proposition 2.5 to the one-edge logarithmic variable t with $M = (\ln b)/2$. □

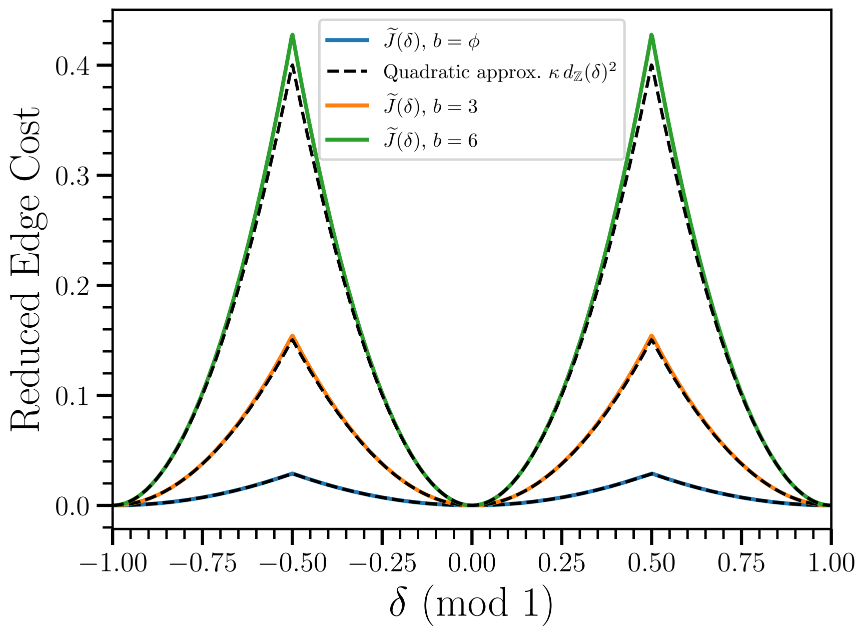

Figure 1: The reduced periodic edge potential $\widetilde{J}_b(\delta)$ for three representative bases $b = 6$, 3, and $\phi = (1+\sqrt{5})/2$. Larger b produces steeper wells. All three curves are 1-periodic, have minima at the integers, and develop cusps at the half-integers because the minimizing lift in (107) changes there.

The quantity $\widetilde{J}_b$ is the one-edge building block of the compactified phase model: once it is known explicitly, the corresponding finite-volume energy is obtained by summing it over edges. Figure 1 displays the periodic well structure, the half-integer cusps, and the dependence on the base b. The harmonic stiffness extracted in Proposition B.6 increases with b through the factor $(\ln b)^2/2$.

The associated local reduced phase energy on a finite graph is

$$\widetilde{C}_{G,b}[\Theta] := \sum_{\langle v,w\rangle \in E} \widetilde{J}_b(\vartheta_v - \vartheta_w), \tag{111}$$

where $\vartheta_v \in \mathbb{R}$ is any lift of $\Theta_v \in \mathbb{R}/\mathbb{Z}$. Because $\widetilde{J}_b$ is 1-periodic, the right-hand side does not depend on the chosen lifts.

For comparison, the genuine graph-level quotient over sitewise integer lifts is

$$Q_{G,b}[\Theta] := \inf_{n\in\mathbb{Z}^V} \sum_{\langle v,w\rangle\in E} \big(\cosh((\ln b)(\vartheta_v - \vartheta_w + n_v - n_w)) - 1\big), \tag{112}$$

which is likewise independent of the chosen lift ϑ.

Proposition B.4 (Local reduction versus graph-level quotient)**.** *For every finite graph G and every phase field $\Theta \in (\mathbb{R}/\mathbb{Z})^V$,*

$$\widetilde{C}_{G,b}[\Theta] \le Q_{G,b}[\Theta]. \tag{113}$$

If G is a tree, equality holds for every Θ. If G contains a cycle, equality need not hold.

Proof. For any $n \in \mathbb{Z}^V$ and any edge $\langle v, w\rangle$,

$$\cosh((\ln b)(\vartheta_v - \vartheta_w + n_v - n_w)) - 1 \ge \widetilde{J}_b(\vartheta_v - \vartheta_w)$$

by the definition (107). Summing over edges and taking the infimum in n gives (113).

Assume now that G is a tree. Choose an orientation of the edges away from a root v_0. For each oriented edge $e = (v, w)$, choose an integer m_e attaining the minimum in $\widetilde{J}_b(\vartheta_v - \vartheta_w)$. Set $n_{v_0} = 0$ and define n_w recursively by $n_v - n_w = m_e$ along every oriented edge. Since G has no cycles, this prescription is consistent and yields an integer field $n \in \mathbb{Z}^V$ realizing every edgewise minimum simultaneously. Hence $Q_{G,b}[\Theta] = \widetilde{C}_{G,b}[\Theta]$.

If G contains a cycle, equality can fail. On the triangle with phase lifts $(\vartheta_1, \vartheta_2, \vartheta_3) = (0, 1/3, 2/3)$, one has

$$\widetilde{C}_{G,b}[\Theta] = 3\big(\cosh((\ln b)/3) - 1\big). \tag{114}$$

For the graph-level quotient, write the three lifted edge differences as

$$\Delta_{12} = -\frac{1}{3} + n_1 - n_2, \qquad \Delta_{23} = -\frac{1}{3} + n_2 - n_3, \qquad \Delta_{31} = \frac{2}{3} + n_3 - n_1,$$

so that $\Delta_{12} + \Delta_{23} + \Delta_{31} = 0$. Each Δ_{ij} lies in $\mathbb{Z} \pm 1/3$, so its absolute value is at least $1/3$. If all three absolute values were $1/3$, then each Δ_{ij} would equal $\pm 1/3$, but no choice of signs on three numbers of magnitude $1/3$ sums to zero. Hence at least one of the three absolute values is at least $2/3$. Since cosh is even and strictly increasing on $[0, \infty)$, the minimum is therefore attained when two edges have absolute value $1/3$ and the third has absolute value $2/3$, namely

$$Q_{G,b}[\Theta] = 2\big(\cosh((\ln b)/3) - 1\big) + \big(\cosh(2(\ln b)/3) - 1\big), \tag{115}$$

which is strictly larger than (114). □

Corollary B.5 (Finite-volume ground states of the reduced compact-phase model)**.** *If G is finite and connected, the minimizers of $\widetilde{C}_{G,b}$ are exactly the constant phase fields $\Theta_v \equiv \Theta_0$.*

Proof. By Proposition B.2, every edge term in (111) is nonnegative and vanishes exactly when adjacent phases agree in $\mathbb{R}/\mathbb{Z}$. Connectedness propagates that agreement across the graph. □

Proposition B.6 (Small-gradient stiffness of the reduced interaction)**.** *For $|\delta| < 1/2$,*

$$\widetilde{J}_b(\delta) = \frac{(\ln b)^2}{2}\,\delta^2 + O(\delta^4) \qquad (\delta \to 0). \tag{116}$$

Thus the harmonic stiffness is

$$\kappa_b = \frac{(\ln b)^2}{2}. \tag{117}$$

Proof. If $|\delta| < 1/2$, then $d_{\mathbb{Z}}(\delta) = |\delta|$, so (109) reduces to $\widetilde{J}_b(\delta) = \cosh((\ln b)\delta) - 1$. The expansion follows from the Taylor series of cosh. □

References

[1] David Ruelle. *Statistical Mechanics: Rigorous Results.* World Scientific, Singapore, 1999.

[2] Barry Simon. *The Statistical Mechanics of Lattice Gases, Volume I.* Princeton University Press, Princeton, NJ, 1993.

[3] Richard S. Ellis. *Entropy, Large Deviations, and Statistical Mechanics*, volume 271 of *Grundlehren der mathematischen Wissenschaften.* Springer, New York, 1985.

[4] R. Tyrrell Rockafellar. *Convex Analysis.* Princeton University Press, Princeton, NJ, 1970.

[5] Sacha Friedli and Yvan Velenik. *Statistical Mechanics of Lattice Systems: A Concrete Mathematical Introduction.* Cambridge University Press, Cambridge, 2017.

[6] Hans-Otto Georgii. *Gibbs Measures and Phase Transitions.* De Gruyter, Berlin, 2 edition, 2011.

[7] Tadahisa Funaki. Stochastic interface models. In *Lectures on Probability Theory and Statistics*, volume 1869 of *Lecture Notes in Mathematics*, pages 103–274. Springer, Berlin, 2005.

[8] Yvan Velenik. Localization and delocalization of random interfaces. *Probab. Surv.*, 3:112–169, 2006. doi: 10.1214/154957806000000050.

[9] Scott Sheffield. Gaussian free fields for mathematicians. *Probab. Theory Relat. Fields*, 139: 521–541, 2007. doi: 10.1007/s00440-006-0050-1.

[10] Sebastian Andres and Peter A. Taylor. Local limit theorems for the random conductance model and applications to the Ginzburg–Landau $\nabla\phi$ interface model. *J. Stat. Phys.*, 182:35, 2021. doi: 10.1007/s10955-021-02705-5.

[11] Pietro Caputo, Cyril Labbé, and Hubert Lacoin. Spectral gap and cutoff phenomenon for the gibbs sampler of $\nabla\varphi$ interfaces with convex potential. *Ann. Inst. H. Poincaré Probab. Statist.*, 58(2):794–826, 2022. doi: 10.1214/21-AIHP1174.

[12] Scott Armstrong and Paul Dario. Quantitative hydrodynamic limits of the Langevin dynamics for gradient interface models. *Electron. J. Probab.*, 29:1–93, 2024. doi: 10.1214/23-EJP1072.

[13] Wei Wu. Local central limit theorem for gradient field models. *Probab. Theory Relat. Fields*, 191:1–40, 2025. doi: 10.1007/s00440-024-01330-z.

[14] Eddy Ardonne, Paul Fendley, and Eduardo Fradkin. Topological order and conformal quantum critical points. *Ann. Phys.*, 310:493–551, 2004. doi: 10.1016/j.aop.2004.01.004.

[15] Herm Jan Brascamp and Elliott H. Lieb. On extensions of the Brunn–Minkowski and Prékopa–Leindler theorems, including inequalities for log concave functions, and with an application to the diffusion equation. *J. Funct. Anal.*, 22:366–389, 1976. doi: 10.1016/0022-1236(76)90004-5.

[16] Ali Naddaf and Thomas Spencer. On homogenization and scaling limit of some gradient perturbations of a massless free field. *Commun. Math. Phys.*, 183:55–84, 1997. doi: 10.1007/BF02505982.

[17] Marek Biskup and Roman Kotecký. Phase coexistence of gradient gibbs states. *Probab. Theory Relat. Fields*, 139:1–39, 2007. doi: 10.1007/s00440-006-0036-0.

[18] Fan R. K. Chung. *Spectral Graph Theory*, volume 92 of *CBMS Regional Conference Series in Mathematics.* American Mathematical Society, Providence, RI, 1997.

[19] Miroslav Fiedler. Algebraic connectivity of graphs. *Czechoslovak Math. J.*, 23:298–305, 1973.

[20] Matthias Keller, Daniel Lenz, and Radosław K. Wojciechowski. *Graphs and Discrete Dirichlet Spaces.* Springer, Cham, 2021.

[21] Reza Olfati-Saber, J. Alex Fax, and Richard M. Murray. Consensus and cooperation in networked multi-agent systems. *Proc. IEEE*, 95:215–233, 2007. doi: 10.1109/JPROC.2006.887293.

[22] Paul Dario. Upper bounds on the fluctuations for a class of degenerate convex $\nabla\phi$-interface models. *ALEA Lat. Am. J. Probab. Math. Stat.*, 21:385–430, 2024. doi: 10.30757/ALEA.v21-17.

[23] Norman Biggs. *Algebraic Graph Theory*. Cambridge University Press, Cambridge, 2 edition, 1993.